Available online at www.sciencedirect.com
ScienceDirect
Solar Energy 84 (2010) 1503–1512
SOLAR ENERGY
www.elsevier.com/locate/solener

Solar absorption cooling plant in Seville

Pablo Bermejo *, Francisco Javier Pino, Felipe Rosa

Departamento de Ingeniería Energética, Universidad de Sevilla, Camino de los Descubrimiento s/n, 41092 Sevilla, Spain

Received 30 October 2009; received in revised form 12 May 2010; accepted 17 May 2010
Available online 11 June 2010

Communicated by: Associate Editor Ruzhu Wang

Abstract

A solar/gas cooling plant at the Engineering School of Seville (Spain) was tested during the period 2008–2009. The system is composed of a double-effect LiBr + water absorption chiller of 174 kW nominal cooling capacity, powered by: (1) a pressurized hot water flow delivered by mean of a 352 m^2 solar field of a linear concentrating Fresnel collector and (2) a direct-fired natural gas burner. The objective of the project is to indentify design improvements for future plants and to serve as a guideline. We focused our attention on the solar collector size and dirtiness, climatology, piping heat losses, operation control and coupling between solar collector and chiller. The daily average Fresnel collector efficiency was 0.35 with a maximum of 0.4. The absorption chiller operated with a daily average coefficient of performance of 1.1–1.25, where the solar energy represented the 75% of generator's total heat input, and the solar cooling ratio (quotient between useful cooling and insolation incident on the solar field) was 0.44.

Keywords: Solar cooling; Double-effect absorption chiller; Linear Fresnel solar collector; Solar cooling ratio; Solar heat fraction

1. Introduction

The current energy systems based on fossil fuels are largely responsible among others for the present humanitarian, environmental and economic crisis. World energy demand – and CO_2 emissions – is expected to rise by some 60% by 2030 respect to the beginning of this century. The EU energy import dependency was 50% in 2000, which is forecasted to increase to approximately 70% by 2030. Due to the fact that reserves of oil and gas are well concentrated, prices are rising gradually (Commission of the European Communities, 2006).

The continued rise in the living and working comfort conditions with reduced prices of air conditioning units are leading to a fast proliferation of these systems, which in residential buildings are low efficiency equipments, with the associated negative impact on electricity demand and environment (ozone layer depletion). In fact, the energy demand for heating is projected to increase until 2030 and then stabilize. In contrast, energy demand for cooling is projected to increase rapidly over the current century due to the climate warming (Isaac and van Vuuren, 2009).

The energy demand in the residential and tertiary sector (services) represents the 36% of European final energy: 25% for households and 11% for services (EUROSTAT, 2010). This amount of energy is mainly used for air conditioning indoor spaces, heating water, electrical appliances and lighting.

These world energy demand trends are the catalysts calling for the creation of new models in heat and power generation; encouraging strategies with renewable energies and higher levels of efficiency to reduce the energy input. In this framework, solar and hybrid technologies represent a potential solution in the near future.

In Seville, the average insolation during warm months (from May to October, both included) is 7.5 kW h/(m^2 day), and 5.5 kW h/(m^2 day) during all year; in the Fig. 1 the average solar direct irradiance during the bright

* Corresponding author.
E-mail addresses: pbm@us.es (P. Bermejo), fjp@us.es (F.J. Pino), rosaif@us.es (F. Rosa).

0038-092X/$ - see front matter © 2010 Elsevier Ltd. All rights reserved.
doi:10.1016/j.solener.2010.05.012

Nomenclature

A_{sc}	solar collector surface (m^2)
c_p	specific heat capacity (J/(kg K))
COP	coefficient of performance
E	energy (W h)
I_d	solar direct irradiance (W/m^2)
HTG	higher temperature generator
LHV_{gas}	natural gas lower heating value (46×10^6 J/kg)
$\dot{m}$	mass flow rate (kg/s)
Q	thermal power (W)
SCR	solar cooling ratio
SHF	solar heat fraction
T	temperature (°C)
UA	heat transfer conductance (W/K)

Greek letters

α	solar azimuth angle (radians)
η	efficiency
ψ	solar elevation angle (radians)

Subscripts

a	absorbed
amb	ambient
$cond$	condenser
$evap$	evaporator
gas	gas
gen	generator
in	inlet
$loss$	loss
out	outlet
p	piping
sc	solar collector
$solar$	solar
sun	sun
w	water

sunshine day length is represented. Thus, Seville and other cities situated in the named Earth's "sun belt" offer an important sustainable energy supply.

The use of solar energy for cooling has the advantage of the synchronization between solar irradiation and cold demand. The two main components of a solar cooling plant are the solar collector and the chiller, where the overall system efficiency depends on the coupling between these two components.

To better understand and compare the solar absorption cooling performances, two ratios should be calculated: (1) the solar cooling ratio (SCR) that represents the efficiency of the complete system, as quotient between the useful cooling and the insolation on the solar field and (2) the solar heat fraction (SHF) that represents the heat injected into the absorption machine generator which is covered by the solar energy:

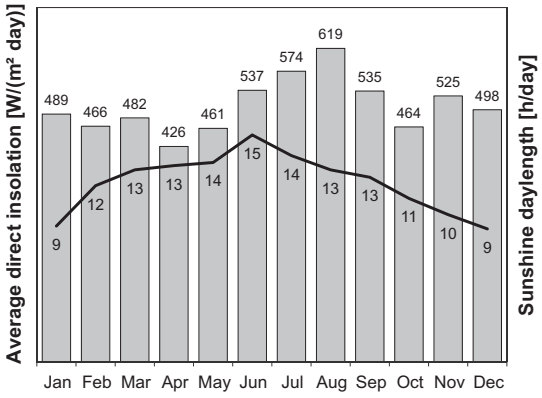

Fig. 1. The bright sunshine direct insolation and its duration in Seville (Departamento de Ingeniería Energética).

$$\mathrm{SCR} = \frac{Q_{evap}}{Q_{sun}}, \tag{1}$$

$$\mathrm{SHF} = \frac{Q_{solar}}{Q_{gen}}. \tag{2}$$

There were 80 large scale solar cooling systems installed around the world in 2007, of which 70 were located in Europe, most of them in Germany and Spain, and 42 of them used absorption machines as chillers (Sparber et al., 2007; Henning, 2007). Fortunately, some projects are being reported and published to create a guideline for future solar cooling plants.

Li and Sumathy (2001) presented the results of a solar powered air conditioning system. The system employed a flat-plate collector array with a surface area of 38 m^2 to drive a single-effect LiBr + water absorption chiller of 4.7 kW cooling capacity and a two partitioned hot water storage tank of 2.75 m^3. The average SCR was about 0.07. Experimental results also showed that during cloudy days, the system could not provide a cooling effect when operated conventionally, however in the partitioned mode-driven system the chiller could be energized, using solar energy as the only heat source.

Syed et al. (2005) reported the performance of a single-effect LiBr + water absorption chiller of 35 kW nominal cooling capacity driven by hot water from a 49.9 m^2 flat-plate collector and 2 m^3 stratified hot water storage tank during hours of bright sunshine. The SCR was about 0.11. The maximum cooling capacity was 7.5 kW (21% of nominal). The measured maximum instantaneous, daily and period averages absorption chiller COP were 0.42 and 0.34, respectively.

Zambrano et al. (2008) presented results of a single-effect LiBr + water of 35 kW nominal cooling capacity

driven by hot water from 151 m^2 flat-plate collector, with an auxiliary gas-fired burner, and 2.5 m^3 stratified hot water storage tank. As a complement to the solar energy, an auxiliary energy system of a gas-fired heater of 60 kW could be used in case solar irradiation was not enough. The SCR was about 0.15, and SHF varied from 0.1 to 1 depending of the solar position.

Ali et al. (2008) reported an air conditioning performance of an integrated free and solar cooling with a single-effect LiBr + water absorption chiller of 34 kW nominal cooling capacity driven by hot water from a 108 m^2 flat-plate collector, a hot water storage capacity of 6.8 m^3, a cold water storage capacity of 1.5 m^3 and a 134 kW cooling tower. The monthly average value of the SHF varied from 0.3 (June and July) to 1 (May, August and September), and the year average value of about 0.6. This novel performance also presents the higher SCR to date with an average value around 0.7.

The single-effect absorption chiller is the most popular due to its low operating temperature. However this plant has a solar collector aperture surface of 352 m^2, much larger than any other reported; reaching and maintaining a water flow at 180 °C to power a double-effect absorption chiller. Hence, this plant represents a forward step in the solar absorption cooling panorama.

The objective of the project is identifying design improvements for possible future plants and to serve as a guideline; where the solar collector size and dirtiness, climatology, heat loss, operation control and coupling between chiller and solar collector are the most important aspects. The plant works on parallel with one megawatt compression cooling equipment for the refrigeration of the building (Monsalvete et al., 2009), and it was monitored during the period 2008–2009 with accompanying optimization of control and operation.

The paper is organized as follow: Section 2 presents a description of the plant, with focus on the solar collector and the chiller as the two main components. Section 3 presents the operational parameters as well as the results of the evaluation during the cold demand season in Seville (May–October): temperatures and heat flows. Section 4 analyses the efficiency of the solar collector and the chiller, as well as the global efficiency of the plant. In Section 5 we analyze some weak points of the plant, a brief economical and emission analysis is also presented. Finally, Section 6 summarize the results obtained during the operation, and examine the potential of this sort of solar cooling plants.

2. Plant description

The solar/gas cooling system installed is a double-effect LiBr + water absorption chiller of 174 kW nominal cooling capacity, powered by: (1) a pressurized hot water flow delivered by mean of a 352 m^2 solar field of a linear concentrating Fresnel collector and (2) a direct-fired auxiliary natural gas burner. The thermal power flows in the system are represented in Fig. 2.

The solar direct radiation incident on the solar field Q_{sun} is concentrated on the absorber tube with a heat net gain $Q_{sc,a}$. The solar collector loss $Q_{sc,loss}$ is due to the temperature difference with ambient (heat loss), and sun position, design, shadows and dirtiness (optical loss). There is a heat loss through the pipeline which connects the solar collector and the absorption chiller $Q_{p,loss}$. The total heat injected into the generator comes from the solar field Q_{solar} and the natural gas burner Q_{gas}. The cooling effect and the energy released out the system are Q_{evap} and Q_{cond} respectively.

2.1. Solar collector

Over the recent years linear concentrating Fresnel solar collectors have attracted a lot of attention within solar heat power production. The slightly curved shape of the reflectors lead to easy construction, production and processing and can therefore be manufactured at low costs. These reflectors occupy a smaller surface area, thus being well suited for installation on flat roofs. In addition, the slightly curved shapes reduce the wind torques over the structure and do not need a particularly solid foundation or a particularly robust support structure, as is the case with a parabolic solar collector.

The sun tracking collectors' efficiency can be expressed as the ratio between net heat absorbed by the thermal-fluid (water) and the direct insolation on the solar field:

$$\eta_{sc} = \frac{Q_{sc,a}}{Q_{sun}} = \frac{\dot{m}_{w,sc} C_{p,w} (T_{sc,out} - T_{sc,in})}{I_d A_{sc}}. \quad (3)$$

The Fresnel solar collector used in our project was manufactured and installed on the roof building by the company PSE AG, which has recently transferred all activities concerning concentrating solar collectors to its newly founded subsidiary Mirroxx GmbH. It consists on a solar field with a total open surface of a 352 m^2 made up of eleven rows of 16 modules (64 m long) that concentrate the sunlight on a tubular vacuum receiver SCHOTT PTR©70 with secondary aluminium CPC concentrator 4 m above the mirror field, see Fig. 3. The thermal-fluid is pressurized overheated water, which is heated up to a maximum operating temperature of 180 °C. The most important characteristics of the solar collector are listed in Table 1.

The solar collector and the absorption chiller are connected by a pipeline of 150 m long. The relative long pipeline represents a weakness in the overall efficiency of the plant due to the pipe-ambient heat loss. Table 2 contains the characteristic of the pipeline circuit.

2.2. Absorption chiller

An absorption cycle is a heat-driven cycle. It exchanges only heat energy with its surroundings and no appreciable mechanical energy is exchanged. In fact, any source of heat can be used: as waste heat fluxes in cogeneration plants (Kalinowski et al., 2009), in combined heat and power system (Trygg and Amiri, 2007) and hot water or steam heat

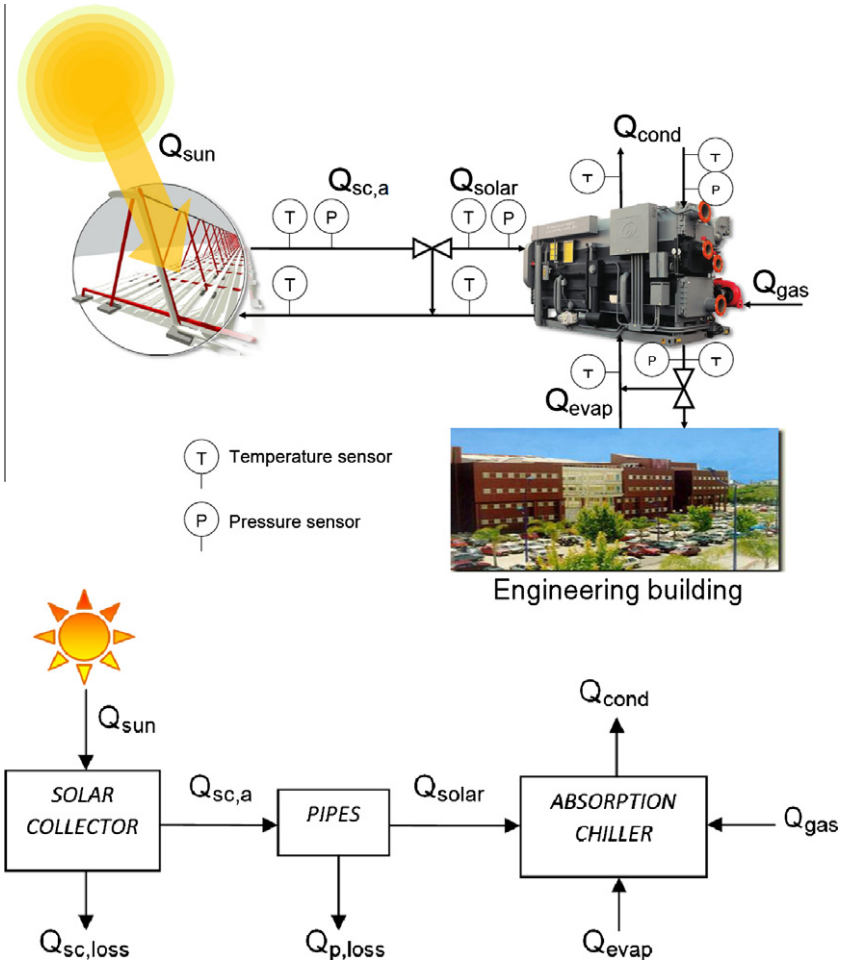

Fig. 2. Scheme and heat flows diagram of the solar/gas absorption cooling plant.

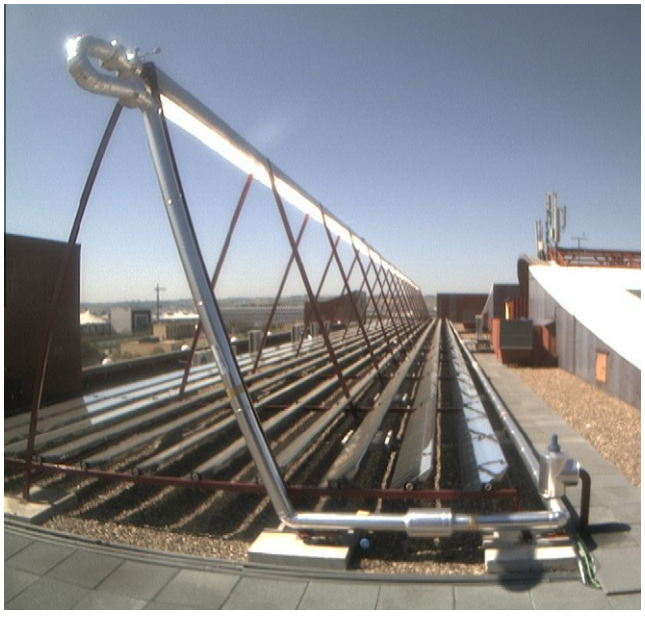

Fig. 3. Linear Fresnel solar collector installed on the roof of the building.

Table 1
Fresnel collector characteristics.

Ground surface	512 m^2
Solar field aperture	352 m^2
Orientation	East–West (18°)
Absorber tube length	64 m
Height of the receiver	4 m
Absorber tube model	SCHOTT PTR©70
Thermal-fluid	Saturated liquid water
Operating temperature	180 °C
Operating pressure	13 bar
Mirror dimension	2 × 0.5 m^2
Numbers of rows	11
Mirror reflectivity	0.92 (clean)
Mirror curvature	8.6–10.6 m

Table 2
Solar piping characteristics.

Inner diameter of pipeline	0.052 m
Outer diameter of pipeline	0.06 m
Total solar circuit length	365 m
Thickness of piping insulator	0.06 m
Heat conductivity of the insulator	0.035 W/(m K)

up in solar collectors (Li and Sumathy, 2001; Syed et al., 2005; Zambrano et al., 2008; Ali et al., 2008).

The absorption cycles require at least two working components: an absorbent and a fluid refrigerant, being LiBr + water and water + NH_3 the most common; although different combinations are being tested such as organic compounds for refrigerants and absorbent. The absorption systems have the advantage in the sense of replacing chlorofluorocarbon (CFC) and hydrochlorofluorocarbons (HCFCs) refrigerants, commonly used in compression chiller systems, and responsible of the ozone layer depletion. The absorption machines operation is well documented (ASHRAE Handbook Fundamentals, 2009).

In Fig. 4 a scheme of a double-effect absorption chiller is shown. The cycle is driven by the energy injected into the generator, the cooling effect is developed in the evaporator and the energy waste is released in the condenser.

The non dimensional number that describe the conversion of heat into cold in the absorption chiller is the COP, defined as the ratio between the useful cooling and the total energy injected into the generator; in this case, from a solar hot water flow and natural gas combustion:

$$\mathrm{COP} = \frac{Q_{evap}}{Q_{gen}} = \frac{\dot{m}_{w,evap} C_{p,w} (T_{evap,in} - T_{evap,out})}{\dot{m}_{w,solar} C_{p,w} (T_{solar,in} - T_{solar,out}) + \dot{m}_{gas} LHV_{gas}}. \quad (4)$$

An important parameter in the absorption chiller is the high temperature generator (HTG); the higher HTG improves the COP and the capacity of the chiller by increasing the refrigerant (water) mass flow rate. The absorption chiller used in this project is the model BROAD-BZH15. The nominal operating parameters are listed in Table 3.

Table 3
Absorption chiller BROAD-BZH15 nominal parameters.

Cooling capacity	174 kW
Temperature evaporator inlet	12 °C
Temperature evaporator outlet	7 °C
Evaporator flow rate	30 m^3/h
Temperature condenser inlet	30 °C
Temperature condenser outlet	37 °C
Condenser flow rate	37 m^3/h
Fuel	Natural gas
HTG	145 °C

The condensation is through a plate heat exchanger with cold water taken from the Guadalquivir River.

3. Operational results

The pilot plant has been running since 2008. The results reported here correspond with the cold demand season in Seville (May–October). The following subsections give temperatures and heat flows of the solar and the absorption chiller.

The operating conditions; such as, temperature and flow rate, are not constant, due to the variation of the solar irradiance throughout the day. As such, they cannot be used directly in order to calculate the thermal power, which in turn prevents the estimation of the solar collector's efficiency and the COP of the chiller. To deal with this, average values have been calculated from experimental measured every twenty seconds for an interval of ten minutes. This method is adequate because the interval exceeds the time it takes for a control volume of water to cross any circuit of the plant.

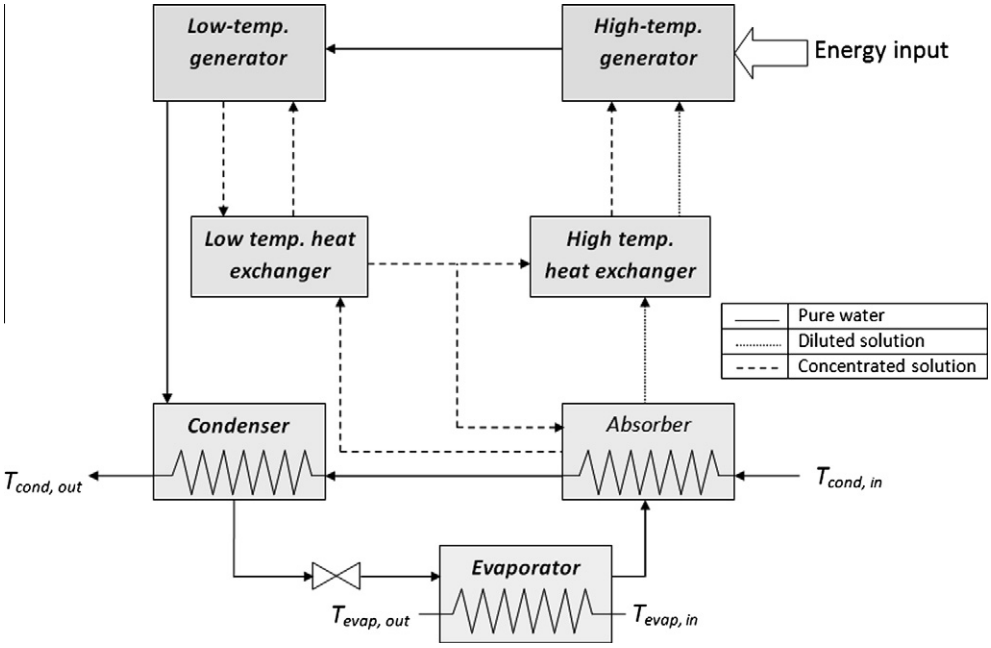

Fig. 4. Double-effect absorption chiller scheme.

3.1. Fresnel collector temperatures

The Fresnel collector starts tracking the sun when solar direct irradiance exceeds 250 W/m^2 to avoid running in cloudy days. The maximum operating temperature is 180 °C. If the temperature exceeds 190 °C, all mirrors shut down by the control system for security reasons.

Fig. 5 shows the collector inlet and outlet temperatures on a typical sunny day. The water flow was 12 m^3/h and the average temperature difference between inlet and outlet was 7.2 °C; this is a solar thermal power of 100 kW, three times higher than the others systems reported (Li and Sumathy, 2001; Syed et al., 2005; Zambrano et al., 2008; Ali et al., 2008). The absorption chiller started working at 12 h; this represented the sudden fall in temperature. That amount of energy was used to warm up the absorption chiller generator. The tracking control took out of focus some mirrors rows, to reduce the aperture surface, hence reduce Q_{sun}; this happened at 13:40 h. Despite the maximum operating temperature of the solar collector is 180 °C, during the test period it was set at 170 °C. For this reason, tracking system regulates when outlet temperature is close to this one and not to 180 °C.

3.2. Absorber tube heat balance

An experimental expression for the solar net heat gained for the water flow through the absorber tube was obtained as difference between irradiance incident on the receiver and its heat loss:

$$Q_{sc,a} = K_1 I_d A_{sc} \sin(\psi) \cos(\alpha) - Q_{sc,loss}. \quad (5)$$

The heat gain, first term in Eq. (5), depends on the solar angles elevation (ψ) and azimuth (α). Therefore, the optical loss is included in this term. The value $K_1 = 0.35$ (statistics covariance = 0.8) was obtained experimentally. On the other hand, the second term represents the heat loss, which depends on the difference of the average absorber tube temperature and ambient temperature.

The heat loss in the receiver was evaluated turning all mirrors out of focus when the solar hot water temperature was 180 °C. Fig. 6 shows a plot of the heat loss $Q_{sc,loss}$ in the Seville Fresnel collector. It is compared with measurements from a previous performance by PSE AG in Palermo (Italy) and measurements of DLR (German Aerospace Centre) for the tubular vacuum receiver SCHOTT PTR©70 (Häberle et al., 2008).

It is acceptable to use a linear approximation for the heat loss over temperature difference:

$$Q_{sc,loss}\,(\mathrm{kW}) = 0.0656(T_{sc} - T_{amb}). \quad (6)$$

The coefficient of expression (5) has been derived from the data collection when the solar collector was operated at steady state. Meanwhile the coefficient of expression (6) was generated by using simple linear regression. Eq. (5) has been tested with 200 operating data points, and predicted experimental heat gain data with a mean absolute error 12%.

We believe the reason why the Seville's collector has a higher heat loss, is the lost of vacuum in some absorber tubes, in fact, ambient moisture condensation within some modules has been observed *in situ*.

3.3. Absorption chiller temperatures

Fig. 7 represents the operating temperatures for the different water flows involved in the absorption chiller. The solar hot water temperature gap (inlet/outlet) was 160/145 °C, condenser gap was 30/36 °C and the evaporator gap was 12/8 °C. The flow rates for condenser and evaporator were nominal 37 and 30 m^3/h, respectively. The absorption chiller was switched on at 12 h, opening the solar heat valve delivering the necessary energy which drives the cycle.

It is observed that there was a cooling effect from when the chiller was switched on, because the low pressure in the evaporator is enough to chill the evaporator water flow,

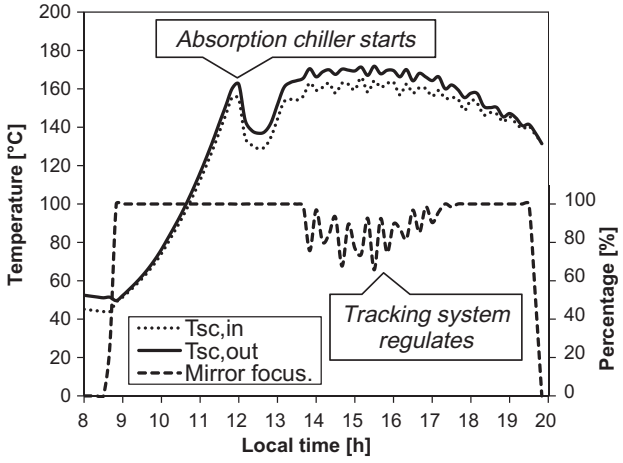

Fig. 5. Solar collector temperatures and percentage of mirrors on focus.

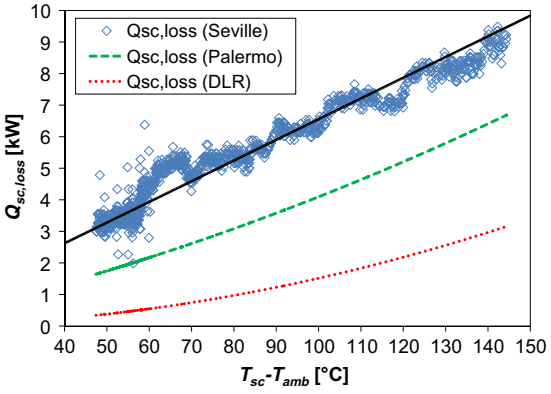

Fig. 6. Heat loss of the absorber tube over temperature difference. Comparison with measurements from two other performances that used SCHOTT PTR©70 receiver.

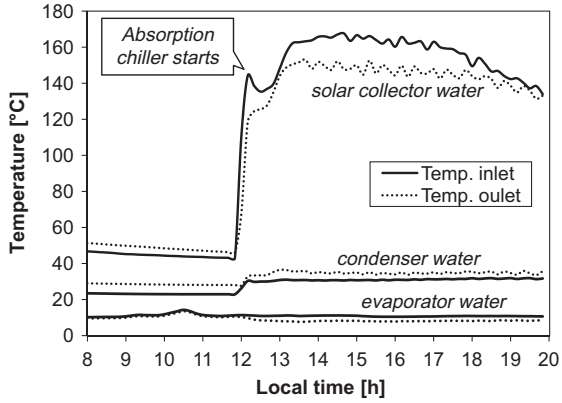

Fig. 7. Absorption chiller water temperatures of the solar collector, condenser and evaporator flows.

and increasing its temperature gap in time when the chiller reaches a steady regime.

3.4. Absorption chiller heat flows

Since the absorption chiller started at 12 h, when the solar water was high enough (160 °C), the control system opened the solar hot water valve to warm the generator and to achieve 145 °C in the HTG. The operating mode gives priority to the solar source rather than to the gas combustion. However, if the HTG is below 145 °C after 30 min from start, the control system turn on the burner, see Fig. 8; this fact happens every day, due to 30 min is not sufficient enough to heat up the generator to 145 °C, despite of the solar hot water temperature could reach 160 °C.

Once reached the steady regime when the HTG was close to 145 °C, the solar hot water delivered by the solar collector represented most of the power introduced into the absorption chiller generator. The cooling power was maintained around 135 kW. Later, when the solar hot water temperature reduced below 150 °C in the afternoon, the gas consumption increased.

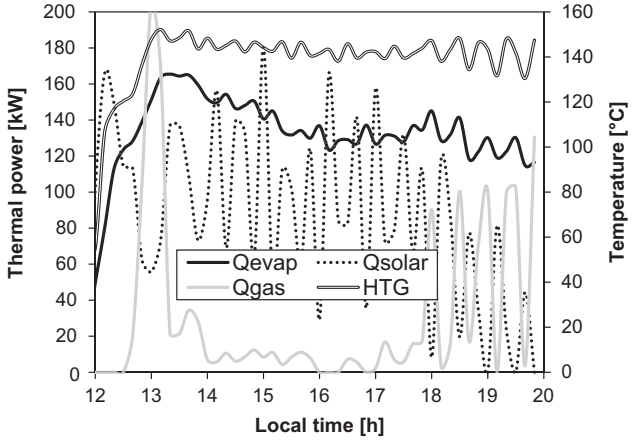

Fig. 8. Generator heat inputs: Q_{solar} and Q_{gas}, cooling power Q_{evap} and HTG.

4. Global balance and efficiency

4.1. Solar collector efficiency

On a sunny day, the average efficiency of the solar collector (using Eq. (3)) was around 0.35, with a maximum of 0.4, see Fig. 9a. On the other hand, when a dust film covers the mirrors, after 3 weeks from the last cleaning, the average efficiency was reduced to 0.16, with a maximum of 0.24, see Fig. 9b.

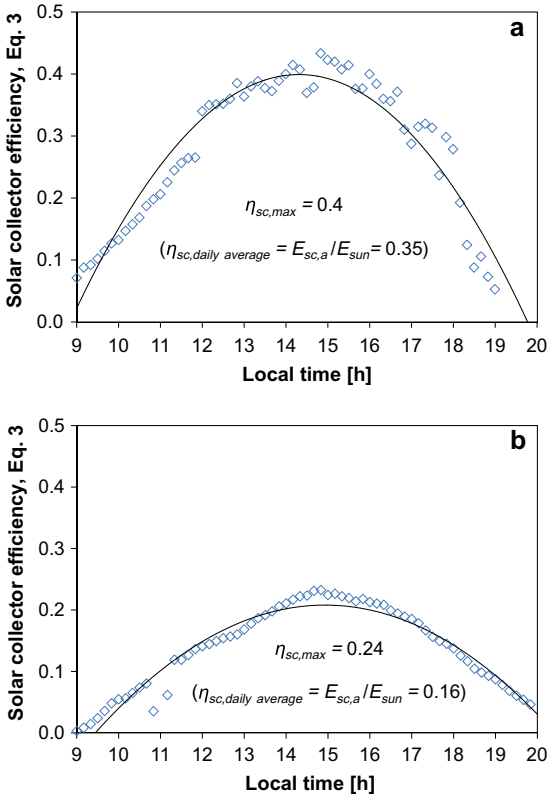

Fig. 9. Daily solar collector efficiency with clean mirrors (a) and dirty mirrors (b).

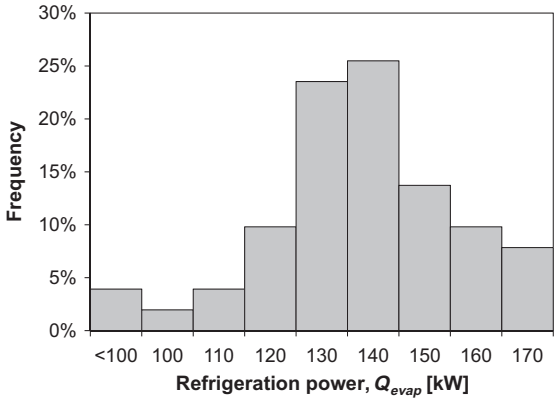

Fig. 10. Histogram of the cooling power on a typical day.

4.2. Absorption chiller: cooling power and COP

The nominal cooling capacity of the absorption chiller installed is 174 kW, with a nominal COP of 1.34. Fig. 10 shows a histogram of the cooling power during a working day, the daily average cooling power was 135 kW (77% of the cooling capacity).

Fig. 11 shows how the COP varied throughout the day. The transient behaviour during the star up period is due to the pressures and temperatures evolution into the different parts of the absorption chiller, also the void fraction in the evaporator and the concentration of the different water. The chiller used in this plant takes around 2 h to achieve the steady regime with maximum COP.

4.3. Global energy balance and efficiency

The daily energy flows diagram in Fig. 12 contains all energy flows in the solar cooling plant on a typical sunny day. The daily average solar collector efficiency was 0.35. The pipeline heat loss represented the 20% of the solar energy absorbed. The COP of the absorption chiller was 1.16. The SHF was 0.75, and the natural gas heat energy supply represented the remaining 0.25. Moreover, the SCR was 0.44.

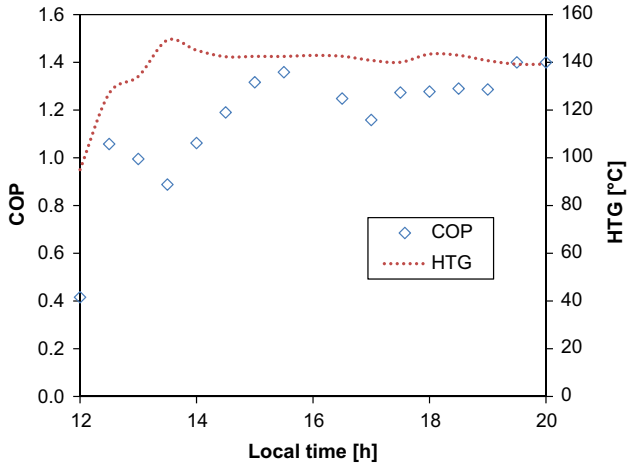

Fig. 11. Absorption chiller COP and HTG variation throughout the day.

5. Discussion

In this section we analyze some weak points of the plant: solar collector size, shades and dirtiness, the heat losses in the pipeline overnight, climatology, lost vacuum in the absorption chiller evaporator, and finally a brief economical and emission analysis is presented.

5.1. Solar collector size, shades and dirtiness

Considering a hypothetical scenario where the absorption chiller operates at 174 kW with a COP of 1.25; the solar energy necessary into the generator would be 140 kW, for no gas consumption. Considering the solar collector efficiency is 0.35. The SHF (considering heat loss in the piping is zero) varies throughout the day with the irradiance. The simulation of a sunny day plotted in Fig. 13 shows that only with a 600 m^2 solar field it is possible to cover all cooling by the solar source for approximate 5 h. The 70 kW h of available energy not used could be storage.

The solar collector efficiency depends on design and other factors, for example sun position (Eq. (5)) or dirtiness. The sun position in the dawn and dusk, with low solar elevation angle, causes that some absorber tube modules in

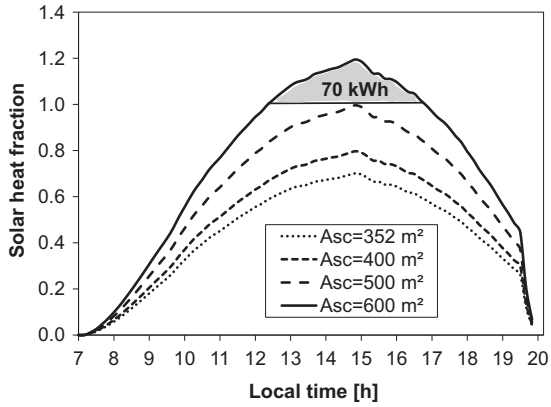

Fig. 13. The solar energy available for cooling depends very notably on the solar field size. Only with a 600 m^2 it is possible to achieve a solar heat fraction equal to one.

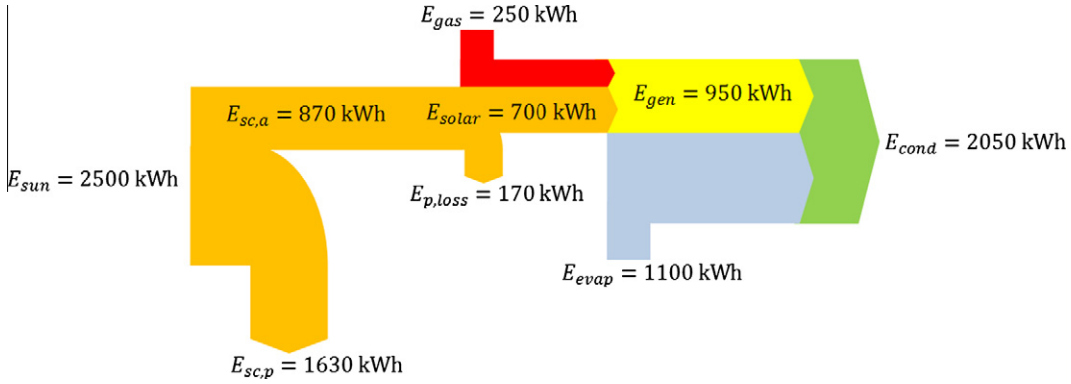

Fig. 12. Daily energy flows diagram (June 23, 2009).

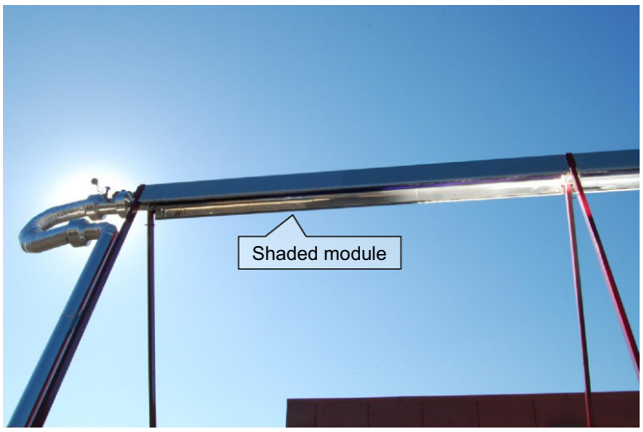

Fig. 14. The east extreme of the absorber tube does not receive solar radiation in the first hours of the morning.

the east and west side respectively, not receive radiation, see Fig. 14; thus more time is needed to achieve the operating temperature, reducing the daily average efficiency. Moreover, when mirrors are dirty, the efficiency is reduced by half. The Fig. 15 compares solar collector temperature when mirrors are clean or dirty: when they are clean, the maximum temperature is achieved early and maintained during most time.

5.2. Heat losses in piping

The surface of the solar collector pipeline (170 m^2) is responsible for a considerable heat waste. In fact, the water mass in the solar collector pipeline reduces its temperature overnight; leading to a morning temperature close to ambient, see Fig. 16. Eq. (7) expresses the average temperature of the solar water in time:

$$T_{w,sc}(t) = T_{amb} + (T_{w,sc}(t=0) - T_{amb}) \exp\left(-\frac{(UA)_p}{m_{w,sc} C_{p,w} t}\right). \quad (7)$$

The piping heat transfer conductance $(UA)_p = 88$ W/K was calculated considering three heat resistances: conduction across steel pipe and insulator and convection plus radiation with the ambient, the internal convection was neglected. The pipeline characteristics are listed in Table 2.

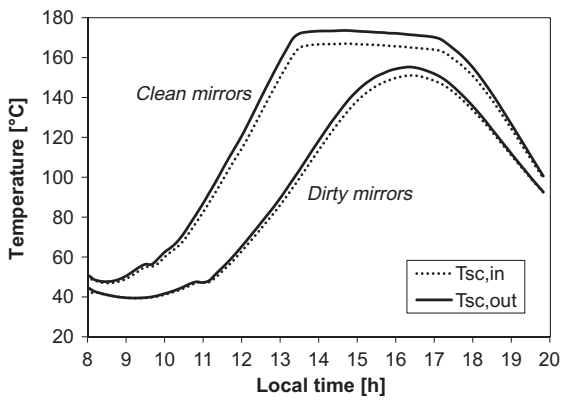

Fig. 15. Comparisons between clean and dirty mirrors.

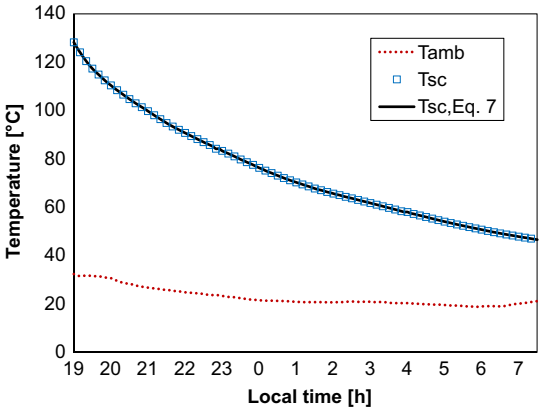

Fig. 16. Solar water heat loss overnight.

Fig. 16 plots the solar hot water overnight; note that water loss 80 °C in 12 h, which is 60 kW h. This nocturnal heat loss is responsible for a start-up delay time of the absorption chiller because the solar collector needs around 3 h to heat up the water, and the absorption chiller generator requires a minimum solar hot water temperature of 145 °C; this represents the 58% of the daily pipeline loss. Therefore an energy storage seems clearly an interesting improve of the system.

5.3. Climatology

If the solar cooling plant runs on a cloudy day, when solar direct irradiance is low and variable, the absorption chiller COP reduces to a unit and solar collector efficiency to 0.25. The gas consumption increases by 60 m^3 (642 kW h), and represents the 60% of the net energy injected into the generator, more than twice for a sunny day (25%).

5.4. Lost vacuum in chiller evaporator

A significant problem during the experimental period was related to the lost vacuum in the absorption machine evaporator. As a consequence of a daily refrigeration cycle, the evaporator increases the pressure, reducing the cooling power to 70 kW (40% of the nominal capacity). The manufacturer's catalogue suggests reducing pressure in the evaporator one time a year; however, it was necessary three times a year in this pilot plant.

5.5. Operation control and coupling between chiller and solar collector. Economical analysis

Because the purpose of the solar cooling plant is to reduce the non-solar energy sources, such as electricity or fossils fuels burning, it is necessary that the absorption chiller starts when the solar hot water temperature is high enough (above 145 °C). The consequent "time delay" is at least of 3 h, due to the overnight piping heat loss.

If the operation mode is only direct-fired, without the solar source, the cooling plant can work all day without

that delay time. But a brief economical analysis proves that this operation mode is more expensive and contaminant than using a compression cooling chiller.

For example, considering a cooling effect of 1 MW h, a compression chiller COP of 3.5 and the absorption chiller COP of 1.1; the input energies necessary are 285 kW h and 909 kW h, respectively.

The current electricity and natural gas costs in Spain are 0.11 €/kW h and 0.05 €/kW h, respectively, therefore the associated costs are 31 € for the compression cooling (285 kW h of electricity) and 45 € for the absorption cooling (909 kW h of gas).

The carbon dioxide emissions associated with the Spanish grid electricity production system is 260 kg of CO_2/MW h (www.ree.es). The natural gas burning emissions are of 194 kg of CO_2/MW h. The CO_2 emissions are 74 kg for the compression chiller and 176 kg for the absorption chiller.

However, this solar/gas absorption cooling plant has an energy cost of 13 € (0.44 times the compression system) and CO_2 emissions associated of 44 kg (0.6 times the compressions system). In short, provided that climatology is favourable, the operational costs is lower in this solar/gas absorption cooling plant than a conventional compression cooling plant, however, a life cycle assessment with payback, amortization, etc. should be done to study the viability.

6. Conclusion

This solar/gas absorption cooling plant has operated 5 days a week during the cold demand season in Seville (May–October). The novel performance here reported is new to date: a double-effect absorption chiller powered by a pressurized hot water flow delivered by mean of a 352 m^2 solar field of a linear concentrating Fresnel solar collector. The main findings can be summarized as follows:

- The daily average linear Fresnel solar collector efficiency was 0.35. But was reduced by half when mirrors were dirty, and the time required to heat up the solar water was greater, see Figs. 9 and 15.
- The absorption chiller worked with a daily average COP of 1.1–1.25. The daily average cooling power was 135 kW (77% of the nominal capacity). However, when there was a lost vacuum in the evaporator, commonplace when the absorption machine works with daily cycles of refrigeration, the cooling power was reduced to 70 kW (40% of the nominal capacity).
- The solar heat fraction was 0.75, and the solar cooling ration was 0.44. These values are really high, and represent a forward step in the solar absorption cooling panorama.
- If the solar cooling plant runs on a cloudy day, the gas consumption increases significantly, representing the 60% of the net energy injected into the generator. Hence, this new performance is only recommended for places with high irradiance and sunny hours. In such cases this solar/gas absorption cooling plant results in a potential energy cost saving with a less environmental impact respect the conventional compression cooling systems.

Acknowledgments

This work has been promoted by the Spanish energy group Gas Natural, with the participation of AICIA and economically supported by Corporación Tecnológica de Andalucía and Junta de Andalucía.

The authors would also like to thank departmental fellow P. Monsalvete for her support on this report.

References

Ali, A.H.H., Noeres, P., Pollerberg, C., 2008. Performance assessment of an integrated free cooling and solar powered single-effect lithium bromide–water absorption chiller. Solar Energy 82, 1021–1030.

ASHRAE Handbook Fundamentals, 2009. 2.13–2.19.

Commission of the European Communities, 2006. Green Paper: A European Strategy for Sustainable, Competitive and Secure Energy, Brussels, COM (2006), vol. 105 Final.

Departamento de Ingeniería Energética, grupo de Termodinámica y Energía Renovables, University of Seville (Spain), meteorological station data collection.

EUROSTAT, 2010.

Häberle, Zahler, C., Luginsland, F., Berger, M., 2008. Practical experience with a linear concentrating Fresnel collector for process heat applications. In: Proceedings of the 14th International Symposium on Concentrated Solar Power and Chemical Energy Technologies, Las Vegas, USA.

Henning, Hans-Martin, 2007. Solar assisted air conditioning of buildings – an overview. Applied Heat Engineering 27, 1734–1749.

Isaac, M., van Vuuren, D.P., 2009. Modeling global residential sector energy demand for heating and air conditioning in the context of climate change. Energy Policy 37, 507–521.

Kalinowski, P., Hwanga, Y., Radermacher, R., Al Hashimi, S., Rodgers, P., 2009. Application of waste heat powered absorption refrigeration system to the LNG recovery process. International Journal of Refrigeration 32, 687–694.

Li, Z.F., Sumathy, K., 2001. Experimental studies on a solar powered air conditioning system with partitioned hot water storage tank. Solar Energy 71, 285–297.

Monsalvete,P., Salmerón, J.M., Bermejo, P., Álvarez, S., Beltrán, M., 2009. Solar refrigeration by absorption in the tertiary sector. In: Proceedings of the 3rd International Conference of Solar Air Conditioning, Palermo, Italy.

Sparber,W., Napolitano, A., Melograno, P., 2007. Overview on the world wide installed solar cooling systems. In: 2nd International Conference Solar Air Conditioning, Tarragona, Spain. <www.iea-shc.org>.

Syed, A., Izquierdo, M., Rodríguez, P., Maidment, G., Missenden, J., Lecuona, A., Tozer, R., 2005. A novel experimental investigation of a solar cooling system in Madrid. International Journal of Refrigeration 28, 859–871.

Trygg, L., Amiri, S., 2007. European perspective on absorption cooling in a combined heat and power system – a case study of energy utility and industries in Sweden. Applied Energy 84, 1319–1337.

Zambrano, D., Bordons, C., Garcia-Gabin, W., Camacho, E.F., 2008. Model development and validation of a solar cooling plant. International Journal of Refrigeration 31, 315–327.